# DANISH METEOROLOGICAL INSTITUTE

## —— SCIENTIFIC REPORT ——

## 02-10

## Canonical Transform Methods for Radio Occultation Data

**Michael E. Gorbunov and Kent B. Lauritsen**

dmi.dk

# Canonical Transform Methods for Radio Occultation Data

Michael E. Gorbunov[1] and Kent B. Lauritsen[2]

[1]*Institute of Atmospheric Physics, Moscow, Russia*
[2]*Danish Meteorological Institute, 2100 Copenhagen, Denmark*

18 November 2002

**Abstract**

In the present work, we study a canonical transform that directly maps the measured field to the impact parameter representation without first carrying out a back-propagation. This canonical transform is determined to first order in a small parameter that measures the deviation of the satellite orbit from a circle. When the parameter is equal to zero, i.e., for circular orbits, then our canonical transform simply reduces to a Fourier transform. In the general case, the form of the generating function is such that it does not directly allow an implementation as an FFT-like algorithm. We are currently investigating the possibility of decomposing the mapping in order to obtain a fast, efficient numerical implementation.

## 1   Introduction

The idea of transforming radio occultation measurements from the space representation to the impact parameter representation was recently shown to be a powerful retrieval method [1]. This transformation is given by a specific canonical transform whose generating function dictates the form of the Fourier integral operator performing the mapping of the field to the ray coordinate representation. It turns out that back-propagation is an immanent part of the canonical transform. Simulations performed with global atmospheric fields for cases with strong water vapor gradients that give rise to multipath propagation show that the canonical transform method can unfold the multipath behavior, thereby leading to more accurate retrieved quantities.
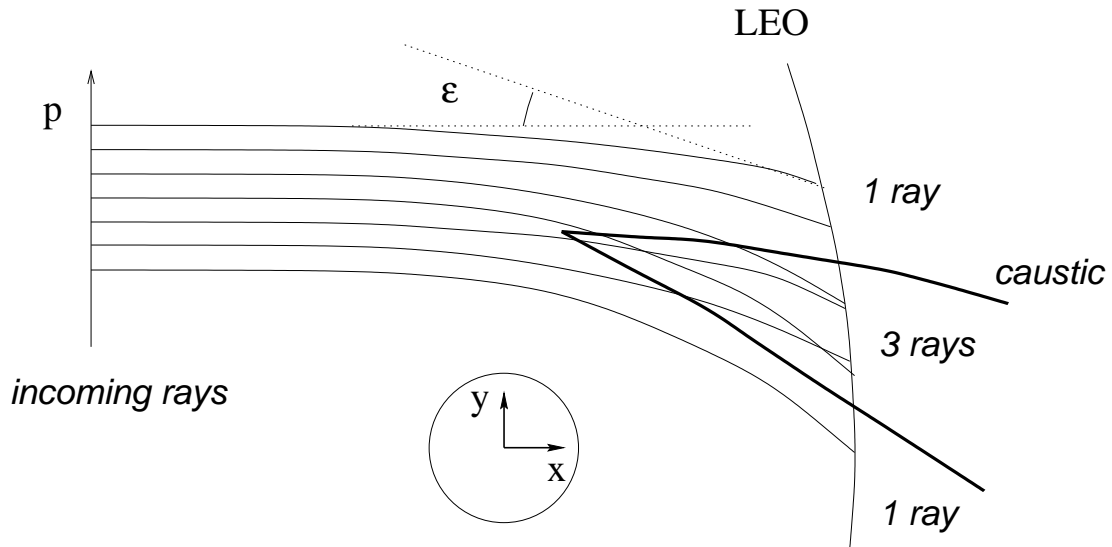
Figure 1: Multipath example: water vapor layers in the lower troposphere give rise to the formation of a caustic (in the example it is a so-called cusp caustic) which surrounds a region with 3 rays passing through any point, implying that 3 rays are arriving at the same time instant at the LEO orbit.

## 2   Multipath

In the present paper we investigate canonical transform (CT) retrieval methods for radio occultations. The geometry $\mathbf{r} = (x, y)$ of the system is chosen such that the $x$-axis coincides with the initial propagation direction of the radio waves (see Fig. 1). For simplicity we can assume the GPS satellite to be located infinitely far away. The origin of the coordinate system is located in the center of curvature of the occultation point. The canonical momentum associated to $y$ is denoted $\eta$. The signal is measured along the low-Earth orbit (LEO) trajectory and we will also refer to this trajectory as a time direction. The impact parameter is denoted $p$ and the bending angle $\epsilon$.

The field measured at the LEO satellite is a solution $u(\mathbf{r}) = A(\mathbf{r}) \exp(i\phi(\mathbf{r}))$ to the Helmholtz equation,

$$\left(\nabla^2 + k^2 n^2(\mathbf{r})\right) u(\mathbf{r}) = 0 , \tag{1}$$

where $k = 2\pi/\lambda$ is the wave-vector of the radio wave emitted from the GPS satellite. The atmosphere is characterized by an index of refraction $n(\mathbf{r})$. In the geometric optics limit $\lambda \rightarrow 0$ we can use the WKB (Wentzel-Kramers-Brillouin) ansatz to
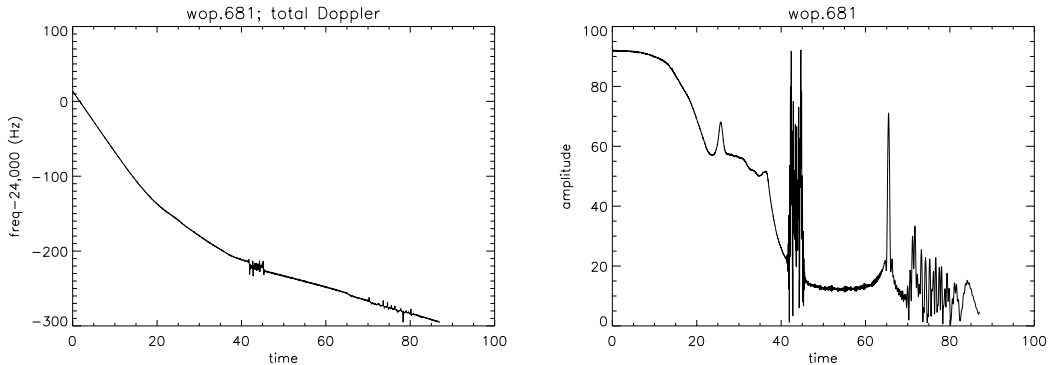
Figure 2: Simulated example (with a wave optics propagator) showing the Doppler (derivative of the phase) and amplitude of a radio signal at the LEO orbit. One observes multipath (MP) behavior with 3 interfering rays appearing around the time 42-46 seconds.

arrive at the solution

$$u(\mathbf{r}) = \frac{1}{\sqrt{j(\mathbf{r})}} \exp\left(ikS(\mathbf{r})\right) . \tag{2}$$

The quantity $S(r)$ is the eikonal and $j(\mathbf{r})$ is the Jacobian of the transformation from $(x, y)$ to ray coordinates and it measures the divergence of a pencil of rays. The points where $j(\mathbf{r}) = 0$, i.e., where the rays tend to focus, define the caustics of the field $u(\mathbf{r})$ (see Figs. 1 and 2) [2].

Since the wavelength is much smaller than typical atmospheric variations, the WKB solution is expected to be a good approximation to the true solution. However, water vapor layers in the troposphere can lead to multipath (MP) propagation implying that the field $u(\mathbf{r})$ will contain caustics. As a result, the WKB solution will breakdown within a region surrounding the caustics. There exists various methods (e.g., uniform approximations, Maslov theory, and Fourier integral operators) to improve the WKB solutions in multipath regions [3].

## 3   Ray Manifold

Figure 3 schematically shows the propagation of rays from the GPS satellite towards the LEO satellite in phase space. Initially, the impact parameter coordinate corresponds to the $y$ coordinate whereas along the LEO orbit one has approximately that the impact parameter is proportional to $\eta$.
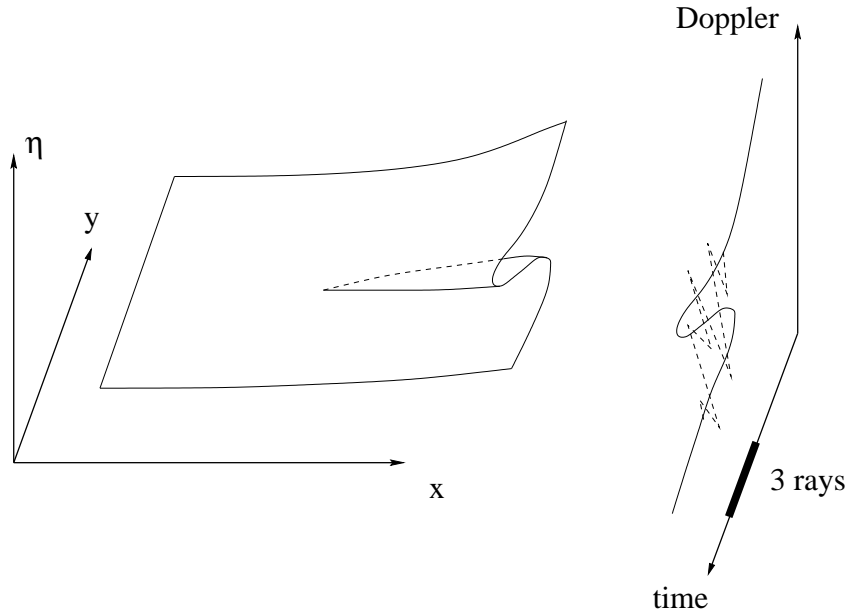
3

Figure 3: Schematic drawing of phase space showing the ray manifold and its projection onto the Doppler vs. time plot. The MP region results in an irregular Doppler signal.

# 4 Canonical Transform with Back-Propagation

We are interested in calculating the bending of individual rays. To this end, one can carry out a transformation of the Helmholtz equation in vacuum to a new set of coordinates that will allow us to extract the ray behavior in multipath regions. The transformation of phase space will be given by a canonical transformation that maps from $(y, \eta)$ to $(z, \xi)$, where $z$ is the new coordinate and $\xi$ its associated canonical momentum [4]. The natural choice of $z$ is the impact parameter $p$ because rays are uniquely defined by their impact parameters for a spherical symmetric atmosphere [1]. This means that MP behavior is unfolded in the $p$-representation (cf. Fig. 4).

Next, we use Egorov's theorem from the theory of Fourier integral operators (FIO) which yields an operator $\Phi_1$ that will transform the field $u$ from the $(y, \eta)$ representation to the $(z, \xi)$ representation [5]. Egorov's theorem states that this mapping is given by the operator

$$\Phi_1 u(z) = \frac{k}{2\pi} \int a_1(z, \eta) e^{ikS_1(z,\eta)} \widetilde{u}_x(\eta) d\eta \,. \tag{3}$$

Here, $a_1(z, \eta)$ is the symbol of the operator and the phase function $S_1(z, \eta)$ is the generating function of the canonical transform discussed below. The field $\widetilde{u}_x(\eta)$ is the Fourier transform of the back-propagated signal $u_x(y)$.
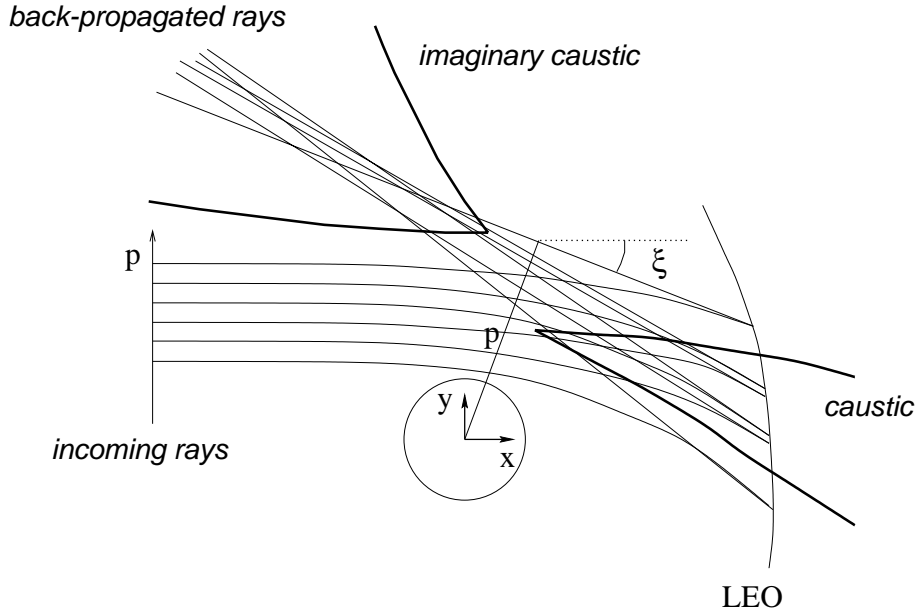
4

Figure 4: Schematic drawing of back-propagation and $(p, \xi)$-representation.

The Fourier transform (FT) is defined by the following equation:

$$Ff(\eta) = \widetilde{f}(\eta) = \int e^{-iky\eta} f(y) dy \,, \tag{4}$$

and the inverse Fourier transform reads

$$F^{-1}\widetilde{f}(y) = f(y) = \frac{k}{2\pi} \int e^{iky\eta} \widetilde{f}(\eta) d\eta \,. \tag{5}$$

It can be noted that the generating function $S_1(z, \eta) = z\eta$ yields a canonical transform which is the identity, and the associated Fourier integral operator is also the identity. The generating function $S(z, \eta) = x\sqrt{1 - \eta^2} + z\eta$ can be shown to give rise to a Fourier integral operator which corresponds to the back-propagation method [1]. The canonical transform recently investigated in [1] is characterized by the generating function

$$S_1(z, \eta) = z \arcsin \eta - x\sqrt{1 - \eta^2}. \tag{6}$$

The new phase space coordinates read

$$z = -x\eta + y\sqrt{1 - \eta^2} \,, \tag{7}$$

$$\xi = \arcsin \eta \,, \tag{8}$$

5

which means that the new coordinate $z$ is the impact parameter $p$ of the ray from the GPS satellite, and $\xi$ is the ray direction angle with respect to the $x$-axis, i.e., $-\xi$ is simply the bending angle $\epsilon$ (note, when the GPS satellite is located at a finite distance a correction term has to be included).

The transformed wave function $\Phi_1 u(p)$ has the WKB form

$$\Phi_1 u(p) \approx A(p) \exp\left(ik \int_{p_0}^{p} \xi(p')dp'\right), \tag{9}$$

where the canonical momentum can be obtained as follows:

$$\xi(p) = \frac{1}{k}\frac{d}{dp} \arg \Phi_1 u(p). \tag{10}$$

## 5  Setting the Scene

We will now discuss the geometry shown in Fig. 5. The equation for the impact parameter reads:

$$p = r\cos\gamma = r\cos(\alpha + \beta) = r\eta\cos\beta + r\sqrt{1-\eta^2}\sin\beta, \tag{11}$$

where the wave vector along the LEO orbit is given by $\eta = \cos\alpha$. Note, in the following $y$ denotes the arc length coordinate along the LEO orbit and $\eta$ is the associated canonical momentum.

Note, one can obtain the following estimates of relevant physical quantities:

- analyses of GPS/MET orbits show that $\beta$ is of the order of $10^{-4} - 10^{-3}$ radians with a variation of about $10^{-4}$ during an occultation.

- the distance $r$ to the LEO orbit varies by about 100 meters during an occultations.

- the order of MP effects on the (total) Doppler can be estimated to be about 3 Hz (corresponding to a deviations of $\frac{1}{3} \times 10^{-3}$ radians of MP rays).

- the effect of non-circular orbits results in a shift of the Doppler frequency of the order of 1 Hz.
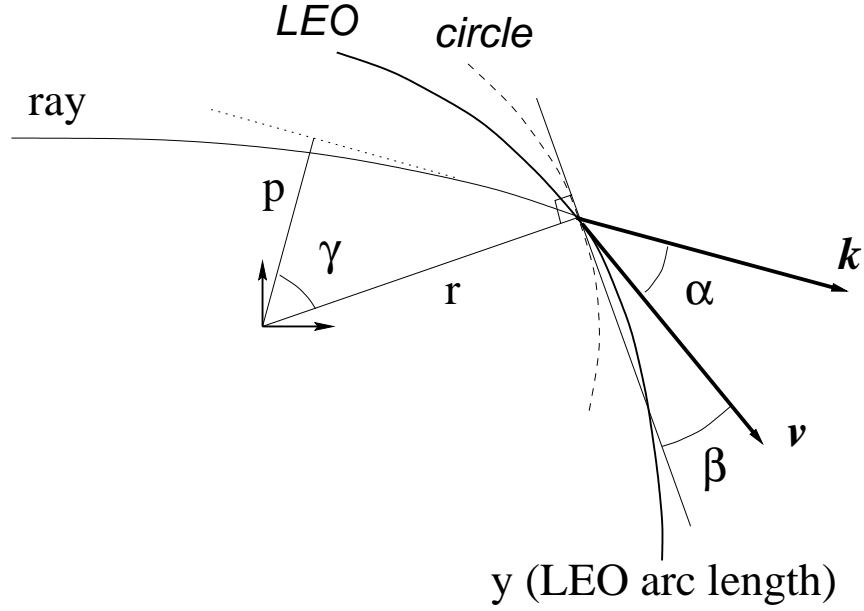
Figure 5: Definition of the angles $\alpha$, $\beta$ and $\gamma$. Note, along the LEO orbit arc length $y$ we have $\eta = \cos \alpha$.

# 6 Canonical Transform without Back-Propagation

In order to proceed, we will assume that $\beta = $ const (which is much smaller than unity). This implies that we take $r(y) = r_0 + \beta(y - y_0)$, where $y_0$ is some reference point which can be chosen in the middle of the MP region. In the following we will take $y_0 = 0$.

The structure of our CT approach is as follows:

- Perform a CT using the field $u(y)$ along the LEO orbit: transform from $(y, \eta)$ to $(z, \xi)$

- FT corresponds to the following: $F$: $z = \eta, \xi = -y$;     $F^{-1}$: $z = -\eta, \xi = y$;

- Egorov's FIO (of type 1):

$$\Phi_1 u(z) = \frac{k}{2\pi} \int a_1(z, \eta) e^{ikS_1(z,\eta)} \widetilde{u_x}(\eta) d\eta \, . \tag{12}$$

The associated generating function is:

$$dS_1 = \xi dz + y d\eta \, . \tag{13}$$

7

- Compose $F^{-1}$ and $\Phi_1$ and obtain a FIO (of type 2):

$$\Phi_2 u(z) = \int a_2(z,y) e^{ikS_2(z,y)} u(y) dy\,, \tag{14}$$

with generating function

$$dS_2 = \xi dz - \eta dy\,. \tag{15}$$

- For the mapping $F$ it follows that $dS_2 = -d(zy)$, i.e., here $\Phi_2$ reduces to a FT: $\Phi_2 u \equiv F u$. Thus, one can think of $\Phi_2$ as a "deformed" FT.

Thus, we seek a CT that maps from $(y,\eta)$ to $(z,\xi)$ with a generating function $S_2 = S_2(z,y)$, where

$$z = p = p(y,\eta)\,, \tag{16}$$

given in Eq. (11). Here, $\xi(y,\eta)$ is to be determined. Then, the transformed wave function $\Phi_2 u(z)$ will unfold MP. It will have the WKB form

$$\Phi_2 u(p) \approx A(p) \exp\left(ik \int_{p_0}^{p} \xi(p') dp'\right)\,, \tag{17}$$

where $\xi = \xi(p)$ follows from the derivative of the phase. Using $y = y(z,\xi)$, one obtains $y(z)$ (and $r(y)$, $\beta(y)$) and this yields the bending angle $\epsilon(p)$.

# 7  Generating Function and New Momentum

Using the canonical formalism (see, e.g., [4]) we obtain the following results (with $y_0 \equiv 0$):

$$z = r_0\eta + y\eta\beta - r_0\sqrt{1-\eta^2}\,\beta + O(\beta^2), \tag{18}$$

$$\xi = -\frac{y}{r_0} + \frac{1}{2}\frac{y^2}{r_0^2}\beta - \beta + \frac{y}{r_0}\frac{\eta}{\sqrt{1-\eta^2}}\beta + O(\beta^2). \tag{19}$$

The generating function reads:

$$S_2(z,y) = -\frac{zy}{r_0} + \frac{1}{2}\frac{zy}{r_0^2}\beta - y\sqrt{1-z^2/r_0^2}\,\beta - z\beta + O(\beta^2). \tag{20}$$

Note the case of circular orbits ($\beta = 0$): This implies, $z = r_0\eta$, i.e., the impact parameter is proportional to the Doppler frequency. In addition, $\xi = -y/r_0$, and $S_2 = -zy/r_0$, i.e., $\Phi_2$ reduces to a Fourier transform in analogy to the full spectrum inversion method [6].

# 8 Conclusions

For a CT of type $\Phi_1$ we have:

    - the structure is symbolically $\Phi_1 \circ F \circ \Phi_{BP} u$

    - both $\Phi_1$ and $F$ can be implemented by FFT-like algorithms

    - the BP transformation reduces diffraction effects in vacuum

This should be compared with a CT of type $\Phi_2$ which is characterized as follows:

    - the structure is $\Phi_2 u$ (i.e., without back-propagation)

    - simple structure, open whether $\Phi_2$ has an FFT-like implementation

    - diffraction effects in vacuum are not completely removed

### Acknowledgements

# References

[1] (i) Gorbunov, M. E.: Radio-holographic analysis of Microlab-1 radio occultation data in the lower troposphere. J. of Geophys. Res., 107(D12), 10.1029/2001JD000889 (2002); (ii) Gorbunov, M. E.: Canonical transform method for processing GPS radio occultation data in lower troposphere. Radio Science (to appear, 2002)

[2] Kravtsov, Y. A., Orlov, Y. I.: Geometrical optics of inhomogeneous media. Springer, Berlin (1990)

[3] Maslov, V. P., Fedoriuk, M. V.: Semi-classical approximations in quantum mechanics. D. Reidel Publishing Company, Dordrecht (1981)

[4] Arnold, V. I.: Mathematical methods of classical mechanics. Springer-Verlag, New York (1978)

[5] Egorov, Yu. V., Komech, A. I., Shubin, M. A.: Elements of the modern theory of partial differential equations. Springer-Verlag, Berlin (1999)

[6] Jensen, A. S., Lohmann, M. S., Benzon, H.-H., Nielsen, A. S., preprint

# DANISH METEOROLOGICAL INSTITUTE

## Scientific Reports

Scientific reports from the Danish Meteorological Institute cover a variety of geophysical fields, i.e. meteorology (including climatology), oceanography, subjects on air and sea pollution, geomagnetism, solar-terrestrial physics, and physics of the middle and upper atmosphere.

Reports in the series within the last five years:

No. 97-1
**E. Friis Christensen og C. Skøtt:** Contributions from the International Science Team. The Ørsted Mission - a pre-launch compendium

No. 97-2
**Alix Rasmussen, Sissi Kiilsholm, Jens Havskov Sørensen, Ib Steen Mikkelsen:** Analysis of tropospheric ozone measurements in Greenland: Contract No. EV5V-CT93-0318 (DG 12 DTEE):
DMI's contribution to CEC Final Report Arctic Tropospheric Ozone Chemistry ARCTOC

No. 97-3
**Peter Thejll:** A search for effects of external events on terrestrial atmospheric pressure: cosmic rays

No. 97-4
**Peter Thejll:** A search for effects of external events on terrestrial atmospheric pressure: sector boundary crossings

No. 97-5
**Knud Lassen:** Twentieth century retreat of sea-ice in the Greenland Sea

No. 98-1
**Niels Woetman Nielsen, Bjarne Amstrup, Jess U. Jørgensen:** HIRLAM 2.5 parallel tests at DMI: sensitivity to type of schemes for turbulence, moist processes and advection

No. 98-2
**Per Høeg, Georg Bergeton Larsen, Hans-Henrik Benzon, Stig Syndergaard, Mette Dahl Mortensen:** The GPSOS project Algorithm functional design and analysis of ionosphere, stratosphere and troposphere observations

No. 98-3
**Mette Dahl Mortensen, Per Høeg:** Satellite atmosphere profiling retrieval in a nonlinear troposphere Previously entitled: Limitations induced by Multipath

No. 98-4
**Mette Dahl Mortensen, Per Høeg:** Resolution properties in atmospheric profiling with GPS

No. 98-5
**R.S. Gill and M. K. Rosengren:** Evaluation of the Radarsat imagery for the operational mapping of sea ice around Greenland in 1997

No. 98-6
**R.S. Gill, H.H. Valeur, P. Nielsen and K.Q. Hansen:** Using ERS SAR images in the operational mapping of sea ice in the Greenland waters: final report for ESA-ESRIN's: pilot projekt no. PP2.PP2.DK2 and 2nd announcement of opportunity for the exploitation of ERS data projekt No. AO2..DK 102

No. 98-7
**Per Høeg et al.:** GPS Atmosphere profiling methods and error assessments

No. 98-8
**H. Svensmark, N. Woetmann Nielsen and A.M. Sempreviva:** Large scale soft and hard turbulent states of the atmosphere

No. 98-9
**Philippe Lopez, Eigil Kaas and Annette Guldberg:** The full particle-in-cell advection scheme in spherical geometry

No. 98-10
**H. Svensmark:** Influence of cosmic rays on earth's climate

No. 98-11
**Peter Thejll and Henrik Svensmark:** Notes on the method of normalized multivariate regression

No. 98-12
**K. Lassen:** Extent of sea ice in the Greenland Sea 1877-1997: an extension of DMI Scientific Report 97-5

No. 98-13
**Niels Larsen, Alberto Adriani and Guido DiDonfrancesco:** Microphysical analysis of polar stratospheric clouds observed by lidar at McMurdo, Antarctica

No. 00-12
**Erik Buch:** A monograph on the physical oceanography of the Greenland waters

No. 00-13
**M. Steffensen:** Stability indices as indicators of lightning and thunder

No. 00-14
**Bjarne Amstrup, Kristian S. Mogensen, Xiang-Yu Huang:** Use of GPS observations in an optimum interpolation based data assimilation system

No. 00-15
**Mads Hvid Nielsen:** Dynamisk beskrivelse og hydrografisk klassifikation af den jyske kyststrøm

No. 00-16
**Kristian S. Mogensen, Jess U. Jørgensen, Bjarne Amstrup, Xiaohua Yang and Xiang-Yu Huang:** Towards an operational implementation of HIRLAM 3D-VAR at DMI

No. 00-17
**Sattler, Kai; Huang, Xiang-Yu:** Structure function characteristics for 2 meter temperature and relative humidity in different horizontal resolutions

No. 00-18
**Niels Larsen, Ib Steen Mikkelsen, Bjørn M. Knudsen m.fl.:** In-situ analysis of aerosols and gases in the polar stratosphere. A contribution to THESEO. Environment and climate research programme. Contract no. ENV4-CT97-0523. Final report

No. 00-19
**Amstrup, Bjarne:** EUCOS observing system experiments with the DMI HIRLAM optimum interpolation analysis and forecasting system

No. 01-01
**V.O. Papitashvili, L.I. Gromova, V.A. Popov and O. Rasmussen:** Northern polar cap magnetic activity index PCN: Effective area, universal time, seasonal, and solar cycle variations

No. 01-02
**M.E. Gorbunov:** Radioholographic methods for processing radio occultation data in multipath regions

No. 01-03
**Niels Woetmann Nielsen; Claus Petersen:** Calculation of wind gusts in DMI-HIRLAM

No. 01-04
**Vladimir Penenko; Alexander Baklanov:** Methods of sensitivity theory and inverse modeling for estimation of source parameter and risk/vulnerability areas

No. 01-05
**Sergej Zilitinkevich; Alexander Baklanov; Jutta Rost; Ann-Sofi Smedman, Vasiliy Lykosov and Pierluigi Calanca**: Diagnostic and prognostic equations for the depth of the stably stratified Ekman boundary layer

No. 01-06
**Bjarne Amstrup**: Impact of ATOVS AMSU-A radiance data in the DMI-HIRLAM 3D-Var analysis and forecasting system

No. 01-07
**Sergej Zilitinkevich; Alexander Baklanov:** Calculation of the height of stable boundary layers in operational models

No. 01-08
**Vibeke Huess**: Sea level variations in the North Sea – from tide gauges, altimetry and modelling

No. 01-09
**Alexander Baklanov and Alexander Mahura**: Atmospheric transport pathways, vulnerability and possible accidental consequences from nuclear risk sites: methodology for probabilistic atmospheric studies

No. 02-01
**Bent Hansen Sass and Claus Petersen**: Short range atmospheric forecasts using a nudging procedure to combine analyses of cloud and precipitation with a numerical forecast model

No. 02-02
**Erik Buch**: Present oceanographic conditions in Greenland waters

No. 02-03
**Bjørn M. Knudsen, Signe B. Andersen and Allan Gross**: Contribution of the Danish Meteorological Institute to the final report of SAMMOA. CEC contract EVK2-1999-00315: Spring-to.-autumn measurements and modelling of ozone and active species

No. 02-04
**Nicolai Kliem**: Numerical ocean and sea ice modelling: the area around Cape Farewell (Ph.D. thesis)

No. 02-05
**Niels Woetmann Nielsen**: The structure and dynamics of the atmospheric boundary layer

No. 02-06
**Arne Skov Jensen, Hans-Henrik Benzon and Martin S. Lohmann:** A new high resolution method for processing radio occultation data

No. 02-07
**Per Høeg and Gottfried Kirchengast**: ACE+: Atmosphere and Climate Explorer

No. 02-08
**Rashpal Gill**: SAR surface cover classification using distribution matching

No. 02-09
**Kai Sattler, Jun She, Bent Hansen Sass, Leif Laursen, Lars Landberg, Morten Nielsen og Henning S. Christensen**: Enhanced description of the wind climate in Denmark for determination of wind resources: final report for 1363/00-0020: Supported by the Danish Energy Authority

No. 02-10
**Michael E. Gorbunov and Kent B. Lauritsen**: Canonical transform methods for radio occultation data

No. 02-11
**Kent B. Lauritsen and Martin S. Lohmann**: Unfolding of radio occultation multipath behavior using phase models

No. 02-12
**Rashpal Gill**: SAR image classification using fuzzy screening method

No. 02-13
**Kai Sattler**: Precipitation hindcasts of historical flood events

No. 02-14
**Tina Christensen**: Energetic electron precipitation studied by atmospheric x-rays